JACS
JOURNAL OF THE AMERICAN CHEMICAL SOCIETY

Article

pubs.acs.org/JACS

Remarkable Enhancement of Chemiluminescent Signal by Dioxetane–Fluorophore Conjugates: Turn-ON Chemiluminescence Probes with Color Modulation for Sensing and Imaging

Nir Hananya,[†] Anat Eldar Boock,[‡] Christoph R. Bauer,[§] Ronit Satchi-Fainaro,[‡] and Doron Shabat*[,†]

[†]School of Chemistry, Raymond and Beverly Sackler Faculty of Exact Sciences, and [‡]Department of Physiology and Pharmacology, Sackler School of Medicine, Tel Aviv University, Tel Aviv 69978, Israel

[§]Bioimaging Center, University of Geneva, CH-1211 Geneva, Switzerland

Supporting Information

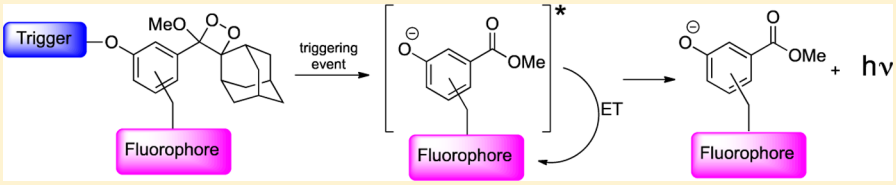

ABSTRACT: Chemiluminescence is among the most sensitive methods for achieving a high signal-to-noise ratio in various chemical and biological applications. We have developed a modular practical synthetic route for preparation of turn-ON fluorophore-tethered dioxetane chemiluminescent probes. The chemiluminescent emission of the probes was significantly amplified through an energy-transfer mechanism under physiological conditions. Two probes were composed with green and near-infrared (NIR) fluorescent dyes tethered to Schaap's dioxetane. While both probes were able to provide chemiluminescence *in vivo* images following subcutaneous injection, only the NIR probe could provide a chemiluminescence image following intraperitoneal injection. These are the first *in vivo* images produced by Schaap's dioxetane chemiluminescence probes with no need of an enhancer. Previously, chemiluminescence cell images could only be obtained with a luciferin-based probe. Our NIR probe was able to image cells transfected with β-galactosidase gene by chemiluminescence microscopy. We also report, for the first time, the instability of dioxetane–fluorophore conjugates to ambient light. Our synthetic route effectively overcomes this limitation through a late-stage functionalization of the dioxetane intermediate. We anticipate that our practical synthetic methodology will be useful for preparation of various chemiluminescent probes for numerous applications.

INTRODUCTION

Chemiluminescence assays are widely utilized in various chemical and biological applications due to their sensitivity and high signal-to-noise ratio.[1,2] Unlike fluorescence-based assays, in chemiluminescence no light excitation is required. Therefore, background signal arising from autofluorescence does not exist when chemiluminescence is used. This circumstance makes chemiluminescence especially useful for tissue and whole-body imaging.[3−6]

Most of the chemiluminescent compounds currently in use are activated by oxidation; i.e., a stable precursor is oxidized, usually by hydrogen peroxide, to form an oxidized high-energy intermediate, which then decomposes to generate an excited species. The latter decays to its ground state by either light emission or energy transfer. Common probes that act on such chemiluminescence mechanisms are usually based on luminol[7] and oxalate esters.[8] Utilizing this oxidation-activated chemiluminescence mode of action, several systems were developed for the *in vivo* imaging of reactive oxygen species (ROS).[9−16] Innately, chemiluminescence that is exclusively activated by oxidation is limited for the detection and imaging of ROS. However, in 1987, Paul Schaap developed a new class of chemiluminescent probes, which can be activated by an enzyme or an analyte of choice.[17−19] Schaap's chemiluminescent probes are based on adamantylidene–dioxetane, triggered through removal of a protecting group from a phenol (Figure 1). The resulting phenolate disassembles via an intramolecular, chemically initiated electron exchange luminescence (CIEEL) mechanism to emit blue light.

In bioassays, under aqueous conditions, Schaap's dioxetanes suffer from one major limitation: their chemiluminescence efficiency decreases significantly through non-radiative energy-transfer processes (quenching) upon interaction with water molecules.[20] A common way to amplify the chemiluminescence signal of Schaap's dioxetanes is through energy transfer from the resulting excited species (the benzoate shown in Figure 1) to a nearby acceptor, which is a highly emissive fluorophore under aqueous conditions.[21,22] Therefore, a surfactant–dye adduct is usually added in commercial chemiluminescent immunoassays. The surfactant reduces water-induced quenching by providing a hydrophobic environment for the excited chemiluminescent probe, which transfers its energy to excite a nearby fluorogenic dye. Consequently, the low-efficiency

Received: September 1, 2016
Published: September 21, 2016

DOI: 10.1021/jacs.6b09173
J. Am. Chem. Soc. 2016, 138, 13438−13446

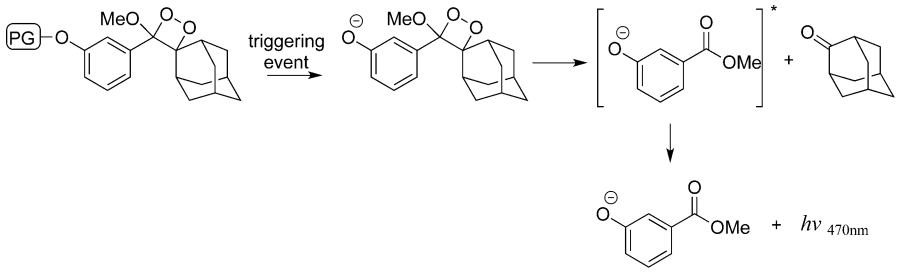

Figure 1. Chemiluminescent activation pathway of Schaap's adamantylidene–dioxetane.

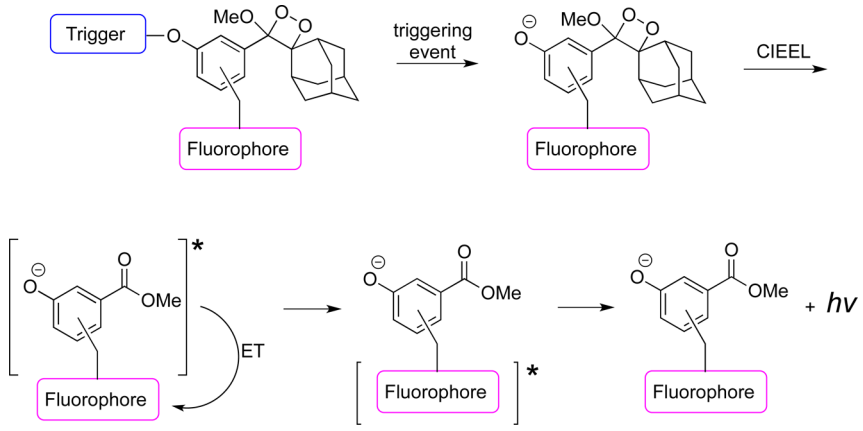

Figure 2. Chemiluminescence activation pathway of dioxetane–fluorophore conjugate.

luminescence process is amplified up to 400-fold in aqueous medium.[23] However, since the surfactant mode of action relies on formation of micelles, its functional concentration is relatively high (above the critical micelle concentration, CMC).[24] As micellar structures are not maintained when animals are treated systemically, the surfactant–dye adduct approach is not practical for *in vivo* detection or imaging of biological activity generated by enzymes or chemical analytes.[25]

To overcome the limitation of a two-component system (a dioxetane probe and a surfactant–fluorescent dye adduct), a single component is required, comprised of dioxetane conjugated with fluorophore. Two previous reports have described synthesis of dioxetane–fluorogenic dye conjugates, in which the dioxetane effectively transfers chemiluminescence energy to the tethered fluorophore to emit light at a wavelength that can be varied by choice of fluorophore.[26,27] In addition to signal amplification, tethering of dioxetane with fluorophore also allows color modulation and red-shifting of the emitted light—a significant requirement for bioimaging applications.[28−33] Herein we report the further elaboration of this approach by developing a more practical synthetic route that solves synthetic restrictions for preparation of dioxetane–fluorophore conjugates. We also report the preparation of the first near-infrared (NIR) Schaap's dioxetane–fluorophore conjugate and demonstrate the applicability of our approach for making chemiluminescence probes suitable for *in vivo* whole-body imaging.

RESULTS AND DISCUSSION

Design and Synthesis of Fluorophore-Tethered Dioxetane Probes. The general structure of the dioxetane–fluorophore conjugate and its activation mechanism are presented in Figure 2. Removal of the trigger by the analyte of interest initiates the CIEEL mechanism, which leads to energy transfer from the excited benzoate to the dye, resulting in excitation of the fluorophore. Thus, light emission should occur from a highly emissive species (the fluorophore) at its corresponding wavelength.

We sought to develop a practical synthetic pathway that allows modular attachment of a fluorophore to the phenolic ring. Dioxetane is usually prepared by reaction of singlet oxygen with a double bond. Since conditions for production of singlet oxygen are not always compatible with the presence of a fluorophore, we developed a late-stage functionalization chemistry that allows attachment of the fluorophore after preparation of the dioxetane. The synthesis of a dioxetane–fluorophore conjugate designed for activation by β-galactosidase (as a model enzyme) is shown in Figure 3. Commercially available aldehyde **1a** was protected with trimethyl orthoformate to give acetal **1b**, followed by additional protection of the phenol group with *tert*-butyldimethylsilyl (TBS) chloride to afford compound **1c**. The latter was reacted with trimethylphosphite to produce phosphonate **1d**, which was condensed with 2-adamantanone via the Wittig–Horner reaction to give enol ether **1e**. Deprotection of the TBS group of **1e** gave phenol **1f**, which was alkylated with a bromo-galactose derivative to afford compound **1g**. Hartwig–Miyaura C–H borylation[34] of **1g** afforded phenylboronic ester **1h**, which was coupled with benzyl bromide **1i** via Suzuki coupling reaction to give compound **1j**. Oxidation of **1j** with singlet oxygen gave *N*-hydroxy-succinimide (NHS)-ester-functionalized dioxetane **1k**. This NHS-ester readily reacts with various amine-functionalized dyes to afford dioxetane–fluorophore conjugate **1m**.

Following the synthetic strategy presented in Figure 3, we prepared three different chemiluminescent probes for monitoring of β-galactosidase activity. The chemical structures of the probes are shown in Figure 4. Probes **2** and **3** are composed of dioxetane tethered with the fluorogenic dyes fluorescein and

DOI: 10.1021/jacs.6b09173
J. Am. Chem. Soc. 2016, 138, 13438−13446

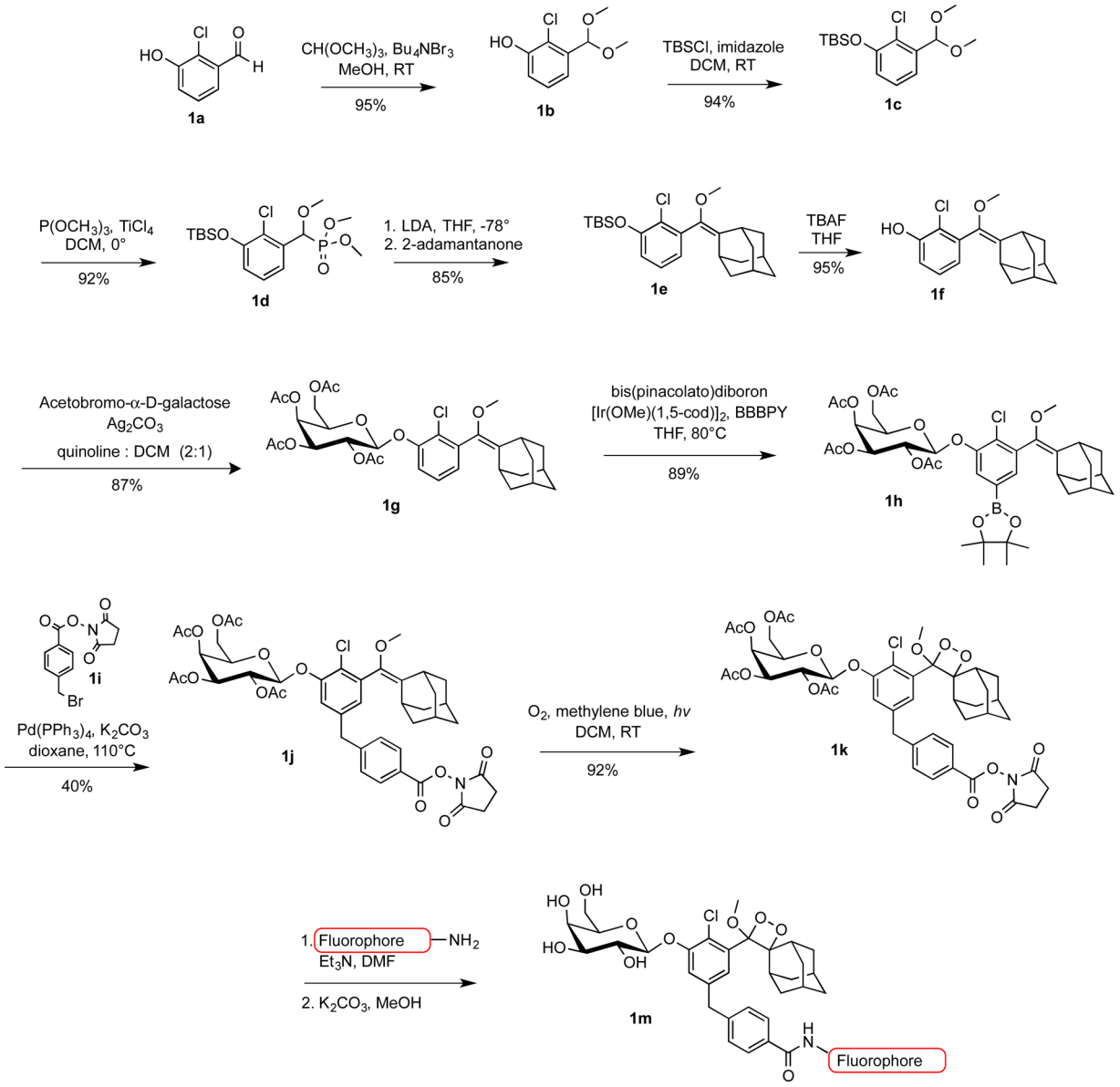

Figure 3. Synthetic strategy for dioxetane–fluorophore conjugates.

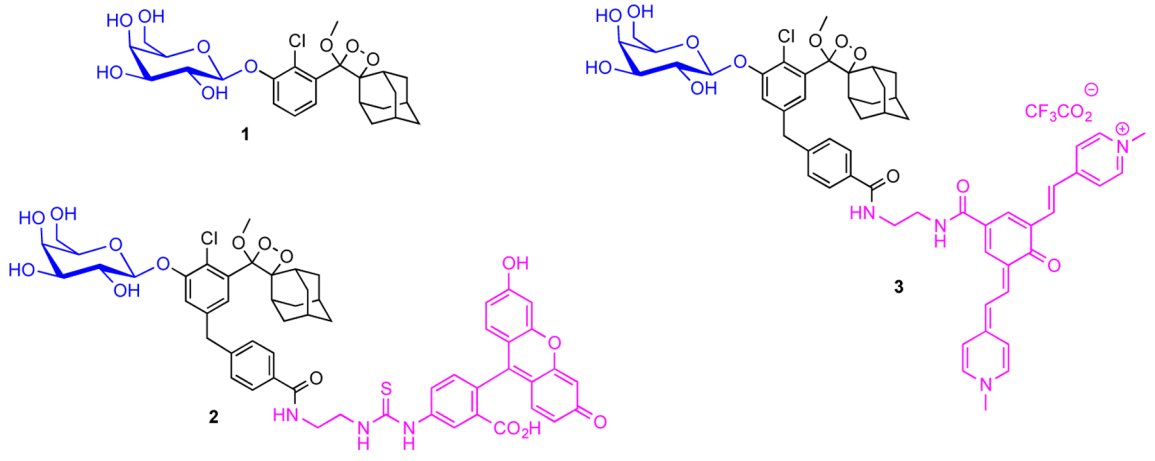

Figure 4. Molecular structures of chemiluminescent probes with emission of three different colors for monitoring of β-galactosidase activity.

quinone-cyanine[35,36] (QCy), respectively. Probe **1** is a basic Schaap-dioxetane without a tethered dye. The chlorine substituent on the phenolic ring was introduced in order to decrease the pK_a of the released phenol after cleavage of the β-

DOI: 10.1021/jacs.6b09173
J. Am. Chem. Soc. 2016, 138, 13438–13446

galactosidase substrate. Such a pK_a should allow the chemiexcitation pathway of the dioxetane to occur under physiological conditions.

Light-Induced Decomposition of Dioxetane−Dye Conjugates. While working on the synthesis of the dioxetane−fluorophore conjugates, we encountered an unexpected phenomenon. Although probe **1** seemed to be photostable, probes **2** and **3** appeared to decompose under normal room illumination conditions. We measured the photostability of the probes in aqueous solution (PBS, pH 7.4) under normal room illumination. The light-induced decomposition was monitored over several hours by a reverse-phase HPLC assay (Figure 5).

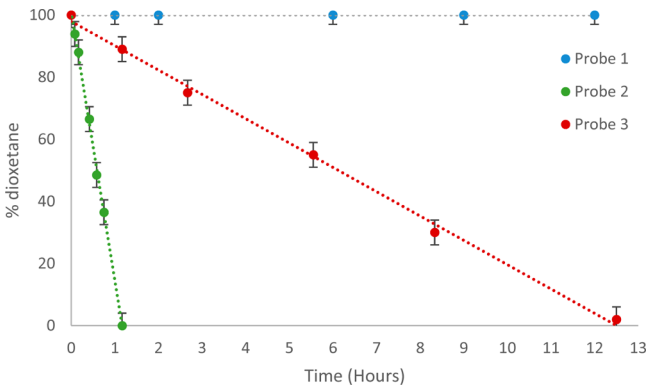

Figure 5. Decomposition of probes **1**, **2**, and **3** under normal room illumination conditions. Probes (300 μM) were incubated in PBS (100 mM), pH 7.4, at ambient temperature.

Probe **1** was unaffected by light over a 12 h period. Probe **3** exhibited significantly higher photostability than probe **2**. The light-induced decomposition half-life of probe **2** was 45 min, whereas the half-life of probe **3** was about 6 h. No decomposition of any of the probes was observed when the solutions were kept in the dark. A possible mechanism for light-induced decomposition of the dioxetane−fluorophore conjugates, might involve electron transfer from the excited dye to the peroxy−dioxetane bond.[48] Figure 6 illustrates a possible light-induced decomposition mechanism. The fluorophore of conjugate **I** is excited by visible light to form excited species **II**. Electron transfer from the LUMO of the excited fluorophore to the antibonding σ^* orbital of O−O peroxide bond results in bond cleavage and subsequent decomposition of the dioxetane into benzoate **III** and adamantanone.

The observed light instability of probes **2** and **3** underlines the advantage of our late-stage functionalization strategy over previous reported synthetic methods for dioxetane−fluorophore conjugates. The oxidation of the enol ether to the dioxetane is usually performed by singlet oxygen generated from oxygen by a light source and a photosensitizer. Such conditions, if applied after the conjugation of the fluorophore, could lead to decomposition of the dioxetane. We were able to avoid light-induced decomposition by using late-stage functionalization chemistry that allows attachment of the fluorophore only after preparation of the dioxetane.

Energy Transfer Observed for Dioxetane−Dye Conjugate vs a Mixture of Dioxetane and a Dye. We first wanted to evaluate the efficiency of energy transfer in the dioxetane−fluorophore conjugates in comparison to a 1:1 mixture of probe **1** and a dye, upon activation with β-galactosidase. The obtained chemiluminescence emission spectra are shown in Figure 7. In the case of fluorescein, two emission maxima were obtained for the dioxetane−dye mixture (Figure 7A) at wavelengths of 470 and 535 nm. These wavelengths correspond to the direct chemiluminescence (DCL) of probe **1** (see Supporting Information) and to the emission of fluorescein resulting from energy transfer (ET), respectively. On the other hand, probe **2** (dioxetane−fluorescein conjugate), upon activation by β-galactosidase, decomposed to emit greenish light with maximum emission wavelength of 535 nm exclusively (Figure 7B). The observed chemiluminescence spectrum of the probe was almost identical to its fluorescence spectrum (dotted line); indicating a complete energy transfer to the fluorescein acceptor. In the case of QCy, only blue emission with maximum wavelength of 470 nm was obtained for the dioxetane−dye mixture (Figure 7C). This emission corresponds to the direct chemiluminescence of probe **1**. On the other hand, probe **3** (QCy-tethered dioxetane) decomposed to emit NIR light with maximum emission wavelength of 714 nm (Figure 7D). Similarly, as observed for probe **2**, the chemiluminescence spectrum of probe **3** was found to be almost identical to its fluorescence spectrum (dotted line). This observation clearly supports the energy transfer mechanism illustrated in Figure 2, and properly demonstrates the significance of covalent conjugation between the dioxetane and the dye.

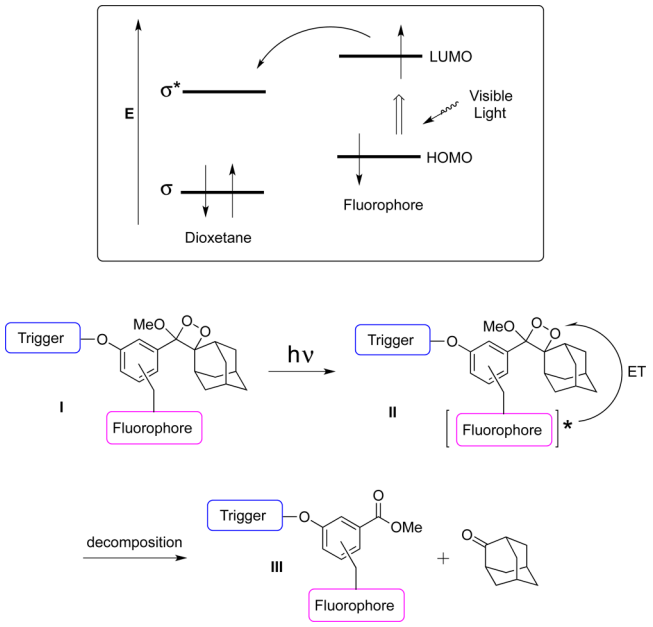

Figure 6. Proposed pathway for visible-light-induced decomposition of dioxetane−fluorophore conjugates.

Chemiluminescence Parameters Measured for Probes 1, 2, and 3 and Their Ability To Detect and Image β-Galactosidase. Next, we measured the light emission of the probes, as a function of time, in the presence and in the absence of β-galactosidase. The probes exhibited a typical chemiluminescent kinetic profile in the presence β-galactosidase with an initial signal increase to a maximum followed by a slow decrease to zero (Figure 8A−C). No light emission was observed from the probes in the absence of β-galactosidase. Figure 8D−F shows the total photon counts emitted from each of the probes. The measured chemiluminescence parameters obtained for probes **1**, **2**, and **3** are summarized in Table 1.

DOI: 10.1021/jacs.6b09173
J. Am. Chem. Soc. 2016, 138, 13438−13446

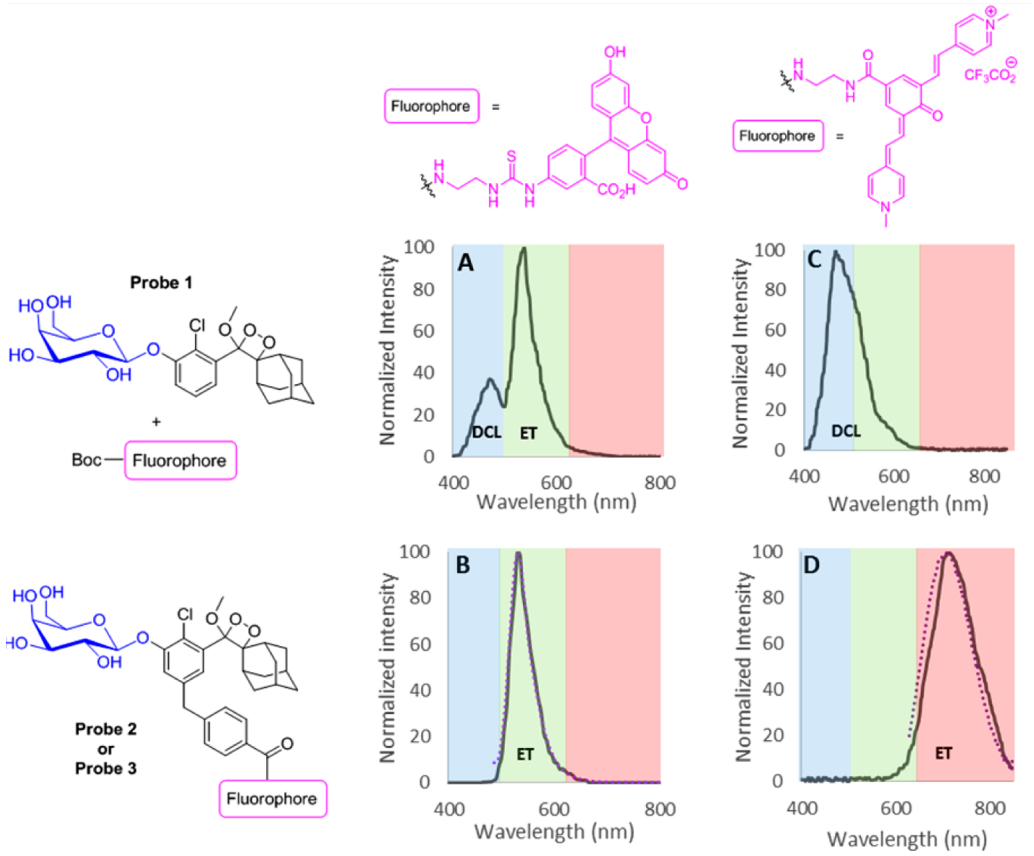

Figure 7. Chemiluminescence emission spectra of 1 μM (A) 1:1 mixture of probe **1** and fluorescein derivative **2b** (see Supporting Information), λ_{max} = 470 nm, 535 nm; (B) probe **2**, λ_{max} = 535 nm; (C) 1:1 mixture of probe **1** and QCy derivative **3b** (see Supporting Information), λ_{max} = 470 nm; and (D) probe **3**, λ_{max} = 714 nm. Spectra were recorded in PBS (100 mM), pH 7.4, in the presence of 1.5 units/mL β-galactosidase (continuous lines). Dotted line is the fluorescence emission spectrum.

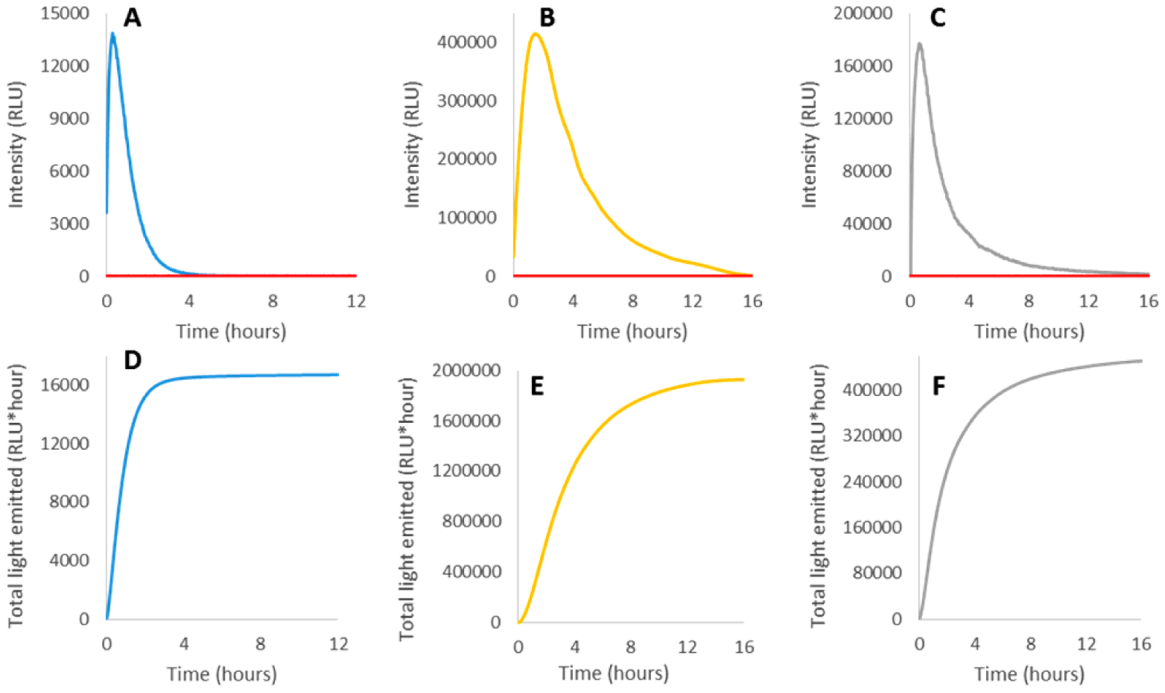

Figure 8. (A–C) Chemiluminescent kinetic profiles of 1 μM (A) probe **1**, (B) probe **2**, and (C) probe **3** in PBS (100 mM), pH 7.4, in the presence of 1.5 units/mL β-galactosidase (blue, yellow, and gray lines, respectively) and in the absence of β-galactosidase (red line). (D–F) Total photon counts emitted from (D) probe **1**, (E) probe **2**, and (F) probe **3** in the presence of β-galactosidase.

DOI: 10.1021/jacs.6b09173
J. Am. Chem. Soc. 2016, 138, 13438–13446

Table 1. Chemiluminescent Parameters Obtained for Probes 1, 2, and 3

probe	λ_{max} (nm)	$T_{1/2}$ (min)	ϕ_{CL}	relative ϕ_{CL}
1	470	40	3.3×10^{-5}	1
2	535	170	3.8×10^{-3}	114
3	714	100	9.0×10^{-4}	27.2

The chemiluminescence quantum yield (ϕ_{CL}) of probes **2** and **3** was calculated using that of probe **1** as a known standard.[37] Probes **2** and **3** exhibited significantly higher light emission than the emission exhibited by probe **1** (114-fold for probe **2** and 27-fold for probe **3**). In addition, probes **2** and **3** had longer half-lives of light emission under identical conditions.

Probe **2** exhibited brighter chemiluminescence than the other probes since its energy transfer is resulted with an excited fluorescein species (a dye with 90% fluorescence quantum yield). We therefore selected probe **2** and demonstrated its ability to detect β-galactosidase (Figure 9). The probe was

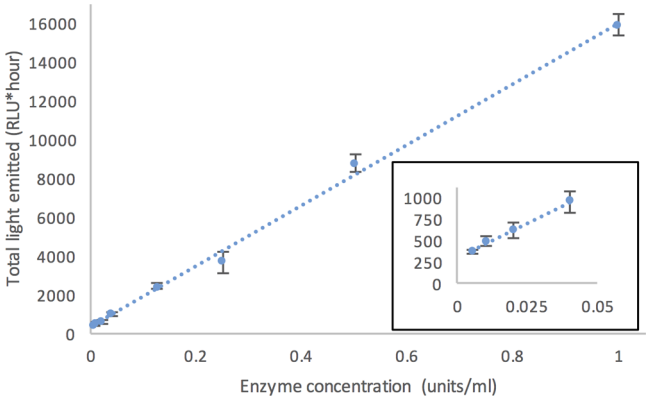

Figure 9. Total light emitted from 10 μM probe **2** in PBS (100 mM), pH 7.4, over a period of 1 h, with different concentrations of β-galactosidase. The inset focuses on light emitted from probe **2** upon incubation with the lowest concentrations of β-galactosidase.

incubated with different concentrations of β-galactosidase and total chemiluminescence emission was collected over 1 h period. Linear correlation was observed between enzyme concentrations and integrated chemiluminescence signal, enabling quantification of enzyme concentration. We determined a detection limit (blank control + 3 SD) of 4.0×10^{-3} units/mL.

The ability of probes **2** and **3** to image β-galactosidase activity was initially evaluated in aqueous solution (PBS, pH 7.4) using probe **1** as a control (Figure 10A). In the absence of β-galactosidase, no chemiluminescence was observed from any of the probes; however, in the presence of the enzyme, probes **2** and **3** emitted light with much stronger intensity than that of probe **1** (about 100-fold for probe **2** and 25-fold for probe **3**, see Figure 10B). Probes **2** and **3** were selected for further evaluation *in vivo*; notably, probe **3** emits light within the near-infrared (NIR) region. This region of light is optimal for *in vivo* imaging applications since NIR photons penetrate organic tissues.[38−43] Probes **2** and **3** were incubated with β-galactosidase and then injected subcutaneously to mice. Under such conditions, clear chemiluminescence images were obtained for both probes (Figure 10C); however, the signal intensity obtained from probe **3** was about 6-fold higher than that obtained from probe **2** (Figure 10D). No chemiluminescence signal was obtained from the probes without pre-incubation with β-galactosidase.

In order to further compare the *in vivo* chemiluminescence signals of probes **2** and **3**, the probes (with and without *ex vivo* incubation with β-galactosidase) were injected into mice via the intraperitoneal route. Remarkably, probe **3** produced a strong chemiluminescence *in vivo* image, whereas no chemiluminescence signal was observed for probe **2** (Figure 11). These observations clearly demonstrate the *in vivo* imaging advantage of the NIR chemiluminescence produced by probe **3** vs that of the green wavelength produced by probe **2**.

In previous examples that used Schaap's dioxetanes for *in vivo* imaging,[44−46] a surfactant−dye adduct (Emerald-II enhancer) was added to the injected solution in order to allow detection of the chemiluminescence signal. The use of multi-component system for *in vivo* imaging has its obvious limitations, especially when the animal is treated systemically. As we demonstrated in Figure 11, bright image was obtained from the QCy-tethered dioxetane (probe **3**), following *ex vivo* activation with β-galactosidase and intraperitoneal injection into mice. Here we established the proof of concept of the dioxetane−fluorophore conjugates to act as turn-ON chemiluminescent probes for *in vivo* imaging. In the next step, we intend to study the capability of the probes to image real pathological events, such as cancer and inflammation. Yet, to demonstrate imaging based on real endogenous activity, we next sought to image cells that endogenously overexpressed β-galactosidase.

Cell Imaging Using Chemiluminescence Microscopy by Probe 3. While fluorescence microscopy is a well-known established method for cell imaging, bioluminescence microscopy has recently been emerged.[47] Instrumentation improvements led to the development of the LV200 microscope by Olympus. The setup of this microscope has significantly improved the ability to localize and quantify luminescence probes at single cell resolution. So far, only luciferin was demonstrated as a probe to image cells transfected by the luciferase gene. We sought to evaluate the ability of probe **3** to image cells with overexpression of β-galactosidase by using the LV200 microscope. HEK293 (transfected by LacZ) and HEK293-WT (control) cells were incubated with probe **3** and then imaged by the LV200 (Figure 12) using a 20× objective (NA 0.75). Probe **3** was able to produce chemiluminescence images of the HEK293-LacZ cells (Figure 12b), while no chemiluminescence signal at all was observed by the HEK293-WT cells (Figure 12d).

To improve the image quality, the HEK293-LacZ cells were fixed by using 4% formaldehyde and permeabilized with 0.1% Triton X-100. The cells were then incubated with probe **3** and imaged by the microscope using a 60× objective (NA 1.42). As can be seen in Figure 13 (a, transmitted light; b, chemiluminescence), the cells became visible, exhibiting a clear chemiluminescence emission.

Although the quality of the obtained images is not high yet, as far as we know, these are the first chemiluminescence cell images produced by a turn-ON small-molecule probe that is not related to luciferin. This approach should allow to image other enzymatic/chemical reactivities in cells by replacing the triggering group of the probe with the appropriate analyte-responsive substrates. The synthetic strategy developed in this work enables convenient synthesis of various chemiluminescence probes. For example, a lipase or an esterase probe can be prepared by incorporation of an appropriate ester triggering

DOI: 10.1021/jacs.6b09173
J. Am. Chem. Soc. 2016, 138, 13438−13446

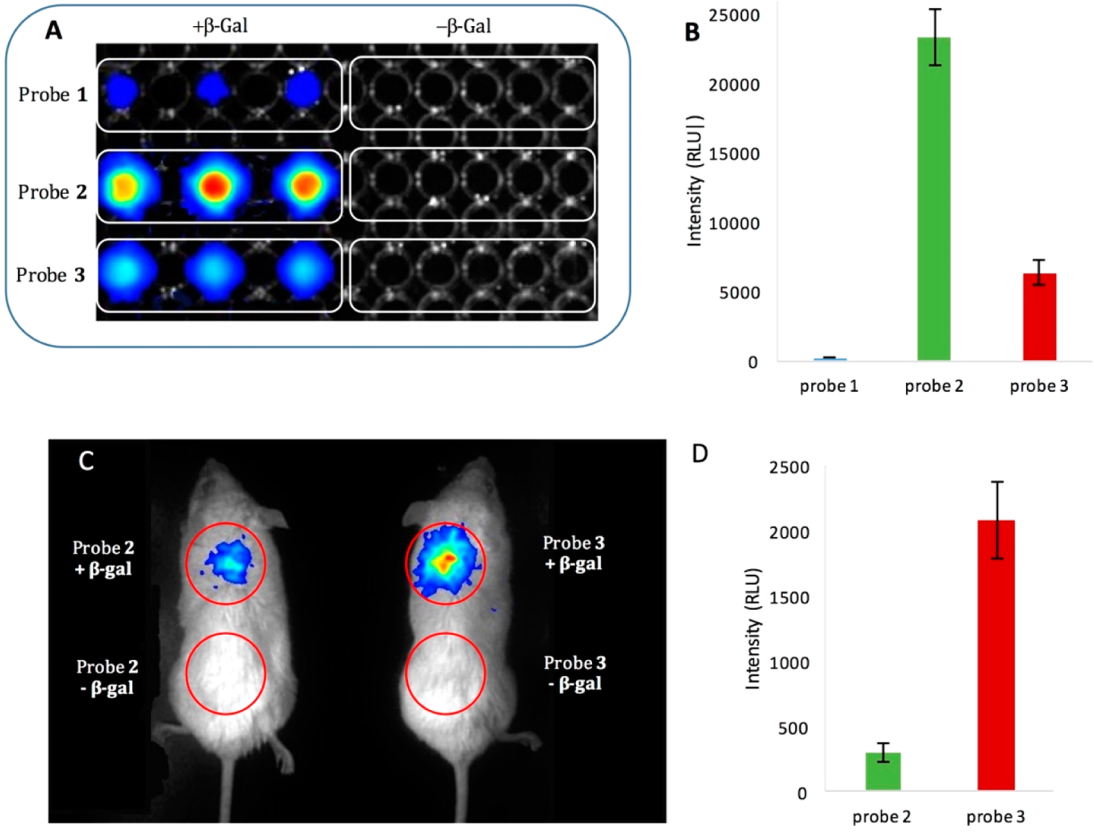

Figure 10. (A) Solution images obtained from 1 μM probes **1**, **2**, and **3** incubated in PBS, pH 7.4, in the presence and in the absence of β-galactosidase. (B) Quantification of signal intensities obtained in solution in the presence of β-galactosidase. (C) Whole-body images obtained 15 min following subcutaneous injection of probes **2** and **3** [50 μL, 1 μM in PBS (100 mM), pH 7.4, after 30 min pre-incubation with or without 1.5 units/mL β-galactosidase]. (D) Quantification of signal intensities in whole-body images in the presence of β-galactosidase (quantitative data are based on repeated imaging experiments with three mice).

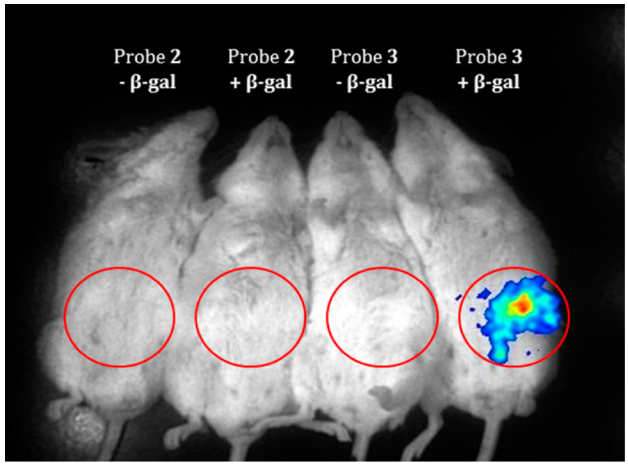

Figure 11. Whole-body images obtained 15 min following intraperitoneal injection of probes **2** and **3** [50 μL, 1 μM in PBS (100 mM), pH 7.4, after a 30 min pre-incubation with or without 1.5 units/mL β-galactosidase].

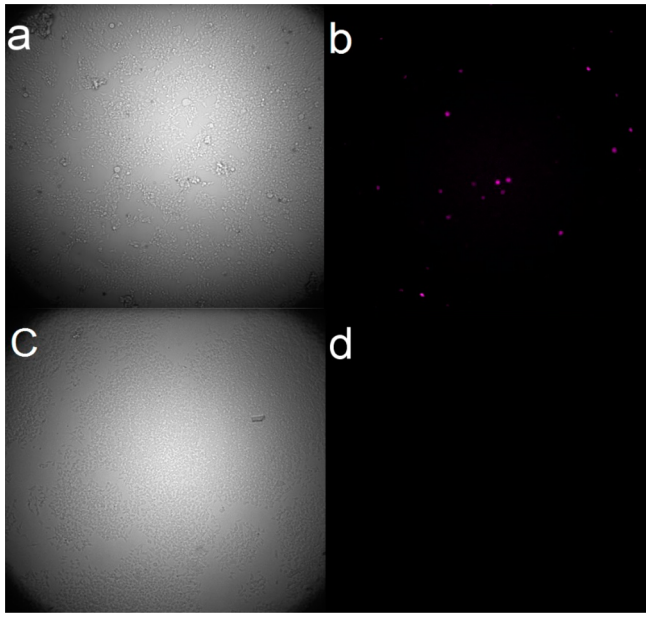

Figure 12. (a) Transmitted light image and (b) chemiluminescence microscopy of HEK293-LacZ stable cells. (c) Transmitted light image and (d) chemiluminescence microscopy of HEK293-WT cells. Images were obtained following 20 min incubation with cell culture medium containing probe **3** (5 μM).

group instead of the β-galactose one. Similarly, the synthesis of proteases probes can be achieved by using a short specific peptide as triggering substrate. Of course, incorporation of certain substrates could be more challenging than others; however, the use of orthogonal protecting groups should assist in solving synthetic difficulties.

DOI: 10.1021/jacs.6b09173
J. Am. Chem. Soc. 2016, 138, 13438−13446

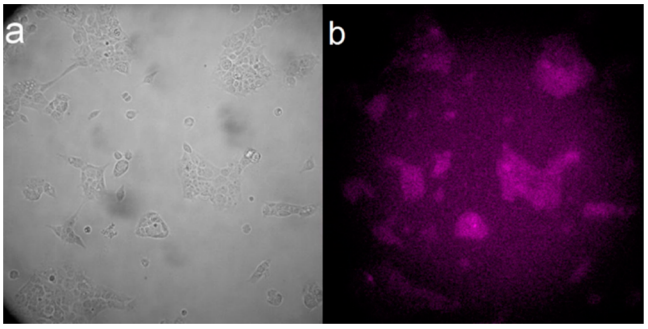

Figure 13. (a) Transmitted light image and (b) chemiluminescence microscopy of HEK293-LacZ stable cells, fixed with formaldehyde (4% for 20 min). Images were obtained following 20 min incubation with cell culture medium containing probe **3** (5 μM).

CONCLUSIONS

In summary, we have developed a simple and practical synthetic route for preparation of turn-ON fluorophore-tethered dioxetane chemiluminescent probes. The effectiveness of the synthesis is based on a late-stage functionalization of a dioxetane precursor by Hartwig–Miyaura C–H borylation, followed by subsequent Suzuki coupling and oxidation to dioxetane. The obtained intermediate is composed of a reactive NHS-ester-dioxetane ready for conjugation with any fluorophore-amine derivative. We also reported the phenomenon of light-induced decomposition of dioxetane–fluorophore conjugates, which highlights the advantage of our synthetic method. The chemiluminescent emission of the fluorophore-tethered dioxetane probes was significantly amplified in comparison to a classic dioxetane probe through an energy-transfer mechanism. The synthesized probes produced light of various colors that matched the emission wavelength of the excited tethered fluorophore. Using our synthetic route, we synthesized two fluorophore-tethered dioxetane probes designed for activation by β-galactosidase and conjugated with green (fluorescein) and NIR (QCy) fluorescent dyes. Both probes were able to provide chemiluminescence *in vivo* images following subcutaneous injection after activation by β-galactosidase. However, a chemiluminescence image following intraperitoneal injection was observed only by the NIR probe. These are the first *in vivo* images produced by Schaap's dioxetane-based chemiluminescence probes with no need of any additive. The NIR probe was also able to image cells, by chemiluminescence microscopy, based on endogenous activity of β-galactosidase. Such probes could be used for *in vivo* imaging of reporter genes, enzymes, and chemical analytes. We anticipate that our practical synthetic methodology for dioxetane-tethered building blocks will be useful for preparation of various chemiluminescent probes suitable for numerous applications.

ASSOCIATED CONTENT

Supporting Information

The Supporting Information is available free of charge on the ACS Publications website at DOI: 10.1021/jacs.6b09173.

Synthetic procedures, characterization data for all new compounds, chemiluminescence spectrum of probe **1**, NMR and MS spectra of probes **1**–**3**, and experimental details of *in vivo* evaluations and cell microscopy imaging (PDF)

AUTHOR INFORMATION

Corresponding Author

*chdoron@post.tau.ac.il

Notes

The authors declare no competing financial interest.

ACKNOWLEDGMENTS

D.S. thanks the Israel Science Foundation (ISF), the Binational Science Foundation (BSF), and the German Israeli Foundation (GIF) for financial support. This work is supported in part by a grant from the Israeli National Nanotechnology Initiative in the Focal Technology Area: Nanomedicines for Personalized Theranostics. R.S.-F. thanks the European Research Council for the ERC Consolidator Grant Agreement no. 617445-PolyDorm.

REFERENCES

(1) Roda, A.; Guardigli, M. *Anal. Bioanal. Chem.* **2012**, *402*, 69.
(2) Roda, A.; Guardigli, M.; Pasini, P.; Mirasoli, M.; Michelini, E.; Musiani, M. *Anal. Chim. Acta* **2005**, *541*, 25.
(3) Gross, S.; Gammon, S. T.; Moss, B. L.; Rauch, D.; Harding, J.; Heinecke, J. W.; Ratner, L.; Piwnica-Worms, D. *Nat. Med.* **2009**, *15*, 455.
(4) Zhang, N.; Francis, K. P.; Prakash, A.; Ansaldi, D. *Nat. Med.* **2013**, *19*, 500.
(5) Van de Bittner, G. C.; Bertozzi, C. R.; Chang, C. J. *J. Am. Chem. Soc.* **2013**, *135*, 1783.
(6) Porterfield, W. B.; Jones, K. A.; McCutcheon, D. C.; Prescher, J. A. *J. Am. Chem. Soc.* **2015**, *137*, 8656.
(7) Merényi, G.; Lind, J.; Eriksen, T. E. *J. Biolumin. Chemilumin.* **1990**, *5*, 53.
(8) Silva, S. M.; Wagner, K.; Weiss, D.; Beckert, R.; Stevani, C. V.; Baader, W. J. *Luminescence* **2002**, *17*, 362.
(9) Lee, D.; Khaja, S.; Velasquez-Castano, J. C.; Dasari, M.; Sun, C.; Petros, J.; Taylor, W. R.; Murthy, N. *Nat. Mater.* **2007**, *6*, 765.
(10) Kielland, A.; Blom, T.; Nandakumar, K. S.; Holmdahl, R.; Blomhoff, R.; Carlsen, H. *Free Radical Biol. Med.* **2009**, *47*, 760.
(11) Lim, C.-K.; Lee, Y.-D.; Na, J.; Oh, J. M.; Her, S.; Kim, K.; Choi, K.; Kim, S.; Kwon, I. C. *Adv. Funct. Mater.* **2010**, *20*, 2644.
(12) Cho, S.; Hwang, O.; Lee, I.; Lee, G.; Yoo, D.; Khang, G.; Kang, P. M.; Lee, D. *Adv. Funct. Mater.* **2012**, *22*, 4038.
(13) Lee, Y.-D.; Lim, C.-K.; Singh, A.; Koh, J.; Kim, J.; Kwon, I. C.; Kim, S. *ACS Nano* **2012**, *6*, 6759.
(14) Shuhendler, A. J.; Pu, K.; Cui, L.; Uetrecht, J. P.; Rao, J. *Nat. Biotechnol.* **2014**, *32*, 373.
(15) Lee, E. S.; Deepagan, V. G.; You, D. G.; Jeon, J.; Yi, G. R.; Lee, J. Y.; Lee, D. S.; Suh, Y. D.; Park, J. H. *Chem. Commun.* **2016**, *52*, 4132.
(16) Li, P.; Liu, L.; Xiao, H.; Zhang, W.; Wang, L.; Tang, B. *J. Am. Chem. Soc.* **2016**, *138*, 2893.
(17) Schaap, A. P.; Handley, R. S.; Giri, B. P. *Tetrahedron Lett.* **1987**, *28*, 935.
(18) Schaap, A. P.; Chen, T.-S.; Handley, R. S.; DeSilva, R.; Giri, B. P. *Tetrahedron Lett.* **1987**, *28*, 1155.
(19) Schaap, A. P.; Sandison, M. D.; Handley, R. S. *Tetrahedron Lett.* **1987**, *28*, 1159.
(20) Matsumoto, M. *J. Photochem. Photobiol., C* **2004**, *5*, 27.
(21) Park, J. Y.; Gunpat, J.; Liu, L.; Edwards, B.; Christie, A.; Xie, X. J.; Kricka, L. J.; Mason, R. P. *Luminescence* **2014**, *29*, 553.
(22) Tseng, J. C.; Kung, A. L. *J. Biomed. Sci.* **2015**, *22*, 45.
(23) Schaap, A. P.; Akhavan, H.; Romano, L. J. *Clin. Chem.* **1989**, *35*, 1863.
(24) Dominguez, A.; Fernandez, A.; Gonzalez, N.; Iglesias, E.; Montenegro, L. *J. Chem. Educ.* **1997**, *74*, 1227.
(25) Torchilin, V. P. *J. Controlled Release* **2001**, *73*, 137.
(26) Schaap, A. P.; Akhavan-Tafti, H. Int. Patent WO 1990007511A1 1990.

DOI: 10.1021/jacs.6b09173
J. Am. Chem. Soc. 2016, 138, 13438–13446

(27) Watanabe, N.; Kino, H.; Watanabe, S.; Ijuin, H. K.; Yamada, M.; Matsumoto, M. *Tetrahedron* **2012**, *68*, 6079.
(28) Matsumoto, M.; Watanabe, N.; Hoshiya, N.; Ijuin, H. K. *Chem. Rec.* **2008**, *8*, 213.
(29) Loening, A. M.; Dragulescu-Andrasi, A.; Gambhir, S. S. *Nat. Methods* **2010**, *7*, 5.
(30) Branchini, B. R.; Ablamsky, D. M.; Rosenberg, J. C. *Bioconjugate Chem.* **2010**, *21*, 2023.
(31) McCutcheon, D. C.; Paley, M. A.; Steinhardt, R. C.; Prescher, J. A. *J. Am. Chem. Soc.* **2012**, *134*, 7604.
(32) Jathoul, A. P.; Grounds, H.; Anderson, J. C.; Pule, M. A. *Angew. Chem., Int. Ed.* **2014**, *53*, 13059.
(33) Steinhardt, R. C.; O'Neill, J. M.; Rathbun, C. M.; McCutcheon, D. C.; Paley, M. A.; Prescher, J. A. *Chem. - Eur. J.* **2016**, *22*, 3671.
(34) Ishiyama, T.; Takagi, J.; Ishida, K.; Miyaura, N.; Anastasi, N. R.; Hartwig, J. F. *J. Am. Chem. Soc.* **2002**, *124*, 390.
(35) Karton-Lifshin, N.; Segal, E.; Omer, L.; Portnoy, M.; Satchi-Fainaro, R.; Shabat, D. *J. Am. Chem. Soc.* **2011**, *133*, 10960.
(36) Karton-Lifshin, N.; Albertazzi, L.; Bendikov, M.; Baran, P. S.; Shabat, D. *J. Am. Chem. Soc.* **2012**, *134*, 20412.
(37) Edwards, B.; Sparks, A.; Voyta, J. C.; Bronstein, I. In *Bioluminescence and chemiluminescence: fundamentals and applied aspects*; Campbell, A. K., Kricka, L. J., Stanley, P. E., Eds.; Wiley: Chichester, 1994; p 56.
(38) Weissleder, R. *Nat. Biotechnol.* **2001**, *19*, 316.
(39) Gnaim, S.; Shabat, D. *Acc. Chem. Res.* **2014**, *47*, 2970.
(40) Redy-Keisar, O.; Kisin-Finfer, E.; Ferber, S.; Satchi-Fainaro, R.; Shabat, D. *Nat. Protoc.* **2014**, *9*, 27.
(41) Kisin-Finfer, E.; Ferber, S.; Blau, R.; Satchi-Fainaro, R.; Shabat, D. *Bioorg. Med. Chem. Lett.* **2014**, *24*, 2453.
(42) Redy-Keisar, O.; Huth, K.; Vogel, U.; Lepenies, B.; Seeberger, P. H.; Haag, R.; Shabat, D. *Org. Biomol. Chem.* **2015**, *13*, 4727.
(43) Redy-Keisar, O.; Ferber, S.; Satchi-Fainaro, R.; Shabat, D. *ChemMedChem* **2015**, *10*, 999.
(44) Cao, J.; Campbell, J.; Liu, L.; Mason, R. P.; Lippert, A. R. *Anal. Chem.* **2016**, *88*, 4995.
(45) Cao, J.; Lopez, R.; Thacker, J. M.; Moon, J. Y.; Jiang, C.; Morris, S. N.; Bauer, J. H.; Tao, P.; Mason, R. P.; Lippert, A. R. *Chem. Sci.* **2015**, *6*, 1979.
(46) Liu, L.; Mason, R. P. *PLoS One* **2010**, *5*, e12024.
(47) Bauer, C. R. *G. I. T. Imaging Microscopy* **2013**, *4*, 32.
(48) Wakimoto, R.; Kitamura, T.; Ito, F.; Usami, H.; Moriwaki, H. *Appl. Catal., B* **2015**, *166−167*, 544.

DOI: 10.1021/jacs.6b09173
J. Am. Chem. Soc. 2016, 138, 13438−13446